G-CSF induced reactive oxygen species involves Lyn-PI3-kinase-Akt and contributes to myeloid cell growth

Quan-sheng Zhu, Ling Xia, Gordon B. Mills, Clifford A. Lowell, Ivo P. Touw, and Seth J. Corey

Granulocyte colony-stimulating factor (G-CSF) drives the production, survival, differentiation, and inflammatory functions of granulocytes. Reactive oxygen species (ROSs) provide a major thrust of the inflammatory response, though excessive ROSs may be deleterious. G-CSF stimulation showed a time- and dose-dependent increase in ROS production, correlating with activation of Lyn and Akt. Inhibition of Lyn, PI3-kinase, and Akt abrogated G-CSF–induced ROS production. This was also blocked by DPI, a specific inhibitor of NADPH oxidase. Following G-CSF stimulation, neutrophils from *Lyn*$^{-/-}$ mice produced less ROSs than wild-type littermates. G-CSF induced both serine phosphorylation and membrane translocation of p47^{phox}, a subunit of NADPH oxidase. Because patients with a truncated G-CSF receptor have a high risk of developing acute myeloid leukemia (AML), we hypothesized that dysregulation of ROSs contributes to leukemogenesis. Cells expressing the truncated G-CSF receptor produced more ROSs than those with the full-length receptor. G-CSF–induced ROS production was enhanced in bone marrow–derived neutrophils expressing G-CSFRΔ715, a truncated receptor. The antioxidant *N*-acetyl-L-cysteine diminished G-CSF–induced ROS production and cell proliferation by inhibiting Akt activation. These data suggest that the G-CSF–induced Lyn-PI3K-Akt pathway drives ROS production. One beneficial effect of therapeutic targeting of Lyn-PI3K-kinase-Akt cascade is abrogating ROS production. (Blood. 2006;107: 1847-1856)

Introduction

Studies on mice deficient in either granulocyte colony-stimulating factor (G-CSF)[1] or its cognate ligand (G-CSF receptor)[2] establish G-CSF as an essential hematopoietic growth factor for the production of granulocytes. As a pleiotropic cytokine, G-CSF promotes the proliferation, survival, differentiation, and end-cell function of granulocytes. The major function of granulocytes is to produce a multipronged defense against microbes, releasing proteases, DNases, and reactive oxygen species (ROSs). Inflammatory cytokines, activated tyrosine kinases, and irradiation produce ROSs.[3-6] G-CSF activates neutrophils to generate superoxide and other forms of ROSs.[7-9] In activated neutrophils as well as in other cell types, the NADPH oxidase generates ROSs.[10] Besides destroying microbes, ROSs can enhance cell growth and transformation,[3] At higher concentrations, ROSs can also trigger the mitochondrial route of caspase activation by forcing open the mitochondrial permeability transition (MPT). This disrupts mitochondrial function and permits cytochrome c release to occur.

Several events must occur to activate NADPH oxidase.[10] On cell stimulation, components of NADPH oxidase assemble with the membrane-bound flavocytochrome b558, which becomes activated and generates O_2^-. NADPH oxidase consists of 6 subunits that are partitioned between different subcellular locations in the resting cells. Two of these subunits, p22^{phox} and gp91^{phox}, are integral membrane proteins and form a heterodimeric flavocytochrome that constitutes the catalytic core of the enzyme. The remaining oxidase components, residing in the cytosol, include the GTPase Rac, p40^{phox}, p47^{phox}, and p67^{phox}. Key to the assembly process is p47^{phox}, a scaffolding molecule that consists of a PX domain, 2 SH3 domains, an arginine/lysine-rich region, and a proline-rich motif. p47^{phox} is responsible for the association of the p40^{phox}, p47^{phox}, p67^{phox} complex with the flavocytochrome because its SH3 domains bind to a proline-rich region in p22^{phox}.[11,12] Patients with autosomally inherited chronic granulomatous disease (CGD) in which no translocation takes place because of a deficiency in p47^{phox}, p67^{phox}, or Rac2 underscore the importance of complete assembly of NADPH oxidase.[13] Thus, a more complete understanding of the signaling processes that drive assembly will be important in designing therapies for inflammatory and other diseases characterized by excessive ROS production.

In angiotensin II–stimulated human smooth muscle cells, Src activation leads to phosphorylation and membrane translocation of p47^{phox}.[14] However, the specific mechanisms whereby Src regulates NADPH oxidase activity have not been identified. Lyn is the predominantly expressed Src family kinase in phagocytic-lineage

From the Division of Pediatrics, University of Texas–M. D. Anderson Cancer Center; the Programs in Cancer Biology and Immunology, University of Texas–M. D. Anderson Cancer Center; the Department of Molecular Therapeutics, University of Texas–M. D. Anderson Cancer Center, Houston; the Department of Laboratory Medicine, University of California at San Francisco; the Department of Hematology, Erasmus University, Rotterdam, The Netherlands; and the Department of Leukemia, University of Texas–M. D. Anderson Cancer Center, Houston.

Submitted April 20, 2005; accepted September 9, 2005. Prepublished online as *Blood* First Edition Paper, November 10, 2005; DOI 10.1182/blood-2005-04-1612.

Supported by the National Institutes of Health (NIH) Independent Scientist Award, NIH grant R29CA74422, American Cancer Society Research Scholar Grant, and Ladies Leukemia League (S.J.C.).

Q.Z. performed the experiments and cowrote the manuscript; L.X. performed the experiments; G.B.M. provided the reagents; C.A.L. created the knock-out mice; I.P.T. created the knock-in mice; and S.J.C. designed the experiments, analyzed the data, and cowrote the manuscript.

Reprints: Seth J. Corey, Section of Pediatric Leukemia/Lymphoma, Box 853, UT–M. D. Anderson Cancer Center, 1515 Holcombe Blvd, Houston, TX 77030; e-mail: sjcorey@mdanderson.org.

The publication costs of this article were defrayed in part by page charge payment. Therefore, and solely to indicate this fact, this article is hereby marked "advertisement" in accordance with 18 U.S.C. section 1734.

cells. G-CSF rapidly activates Lyn, which plays a critical role in cellular proliferation and differentiation.[15-17] Among Lyn's downstream effectors are Akt[17-20] and ERK1/2.[17,21-25] Either Akt[26,27] or ERK1/2[28-31] can phosphorylate p47^{phox} and, therefore, are likely candidates for G-CSF receptor–mediated ROS production. Using wild-type and truncated G-CSF receptor–transfected Ba/F3 and 32D cells, as well as Lyn-deficient and G-CSFRΔ715 knock-in mice, we demonstrated that G-CSF–mediated ROS production is dependent on the Lyn-phosphatidylinositol 3 (PI3)–kinase-Akt pathway by stimulating phosphorylation and membrane translocation of p47^{phox} and subsequent activation of NADPH oxidase. We also found that hyperactivation of Lyn, correlated with enhanced Akt activation, was associated with increased ROS production in Ba/F3 cells expressing truncated G-CSF receptor.

Materials and methods

Reagents

Commercially available antibodies used were to detect phospho-Src Y416, phospho-Lyn Y507, Akt, phospho-Akt S473, phospho-ERK1/2 T202/Y204, p38, phospho-p38 T180Y182, phospho-GSK3 S21/9, mTOR, and phospho-mTOR S2448 (Cell Signaling, Beverly, MA); phospho-serine (Sigma, St Louis, MO); and actin, Lyn, and p47^{phox} (Santa Cruz Biotechnology, Santa Cruz, CA). Anti-GSK3 antibody was purchased from UBI (Lake Placid, NY). The source of human recombinant G-CSF was filgrastim (Amgen, Thousand Oaks, CA). The Src kinase inhibitor PP1was purchased from Affiniti (Exeter, United Kingdom), the PI3-kinase inhibitor Ly294002 was from Cayman Chemical (Ann Arbor, MI), and the MEK1/2 inhibitor was from Calbiochem (Darmstadt, Germany). We obtained from Abbott Laboratories (Abbott Park, IL) the selective Akt inhibitor, 4-amino-2-(3,4-dichlorophenyl)-*N*-(1*H*-indazol-5-yl)-butyramide, which is also known as compound A838450 (international publication no. WO 03/064397 A1). Its observed IC_{50} for Akt-1 is 8 nM, Aurora-2 1400 nM, CDK-2 1300 nM, PKC greater than 40 000 nM, SGK 48 nM, and Src 3900 nM. The antioxidant *N*-acetyl-L-cysteine (NAC) and diphenyleneiodonium chloride (DPI) were purchased from Sigma-Aldrich (St Louis, MO).

Cell lines

Ba/F3, 32D cells, and their derivatives were grown in RPMI medium supplemented with 10% FCS, 2 mM glutamine, 50 U/mL penicillin, 50 μg/mL streptomycin, and 2 ng/mL murine rIL-3 (PeproTech, Rocky Hill, NJ). Different forms of the human G-CSF receptor cDNA with an HA tag were constructed by polymerase chain reaction (PCR) and site-directed mutagenesis techniques and cloned into pcDNA3 vector. Stable transfectants of Ba/F3 cells expressing either wild-type or truncated G-CSF receptor has been described elsewhere.[17]

Purification of murine neutrophils

Lyn-deficient, G-CSFRΔ715 knock-in mice, and their wild-type mice were kept on a 12:12-hour light-dark cycle with free access to food and autoclaved water. The experiments were conducted in accordance with institutional review board-approved protocols at the University of Texas–M. D. Anderson Cancer Center. Male *Lyn*$^{-/-}$ or G-CSFRΔ715 knock-in mice, and their littermate wild-type mice were killed at 12 weeks to obtain femur and tibia. To get bone marrow cell suspension, the femur and tibia were flushed with 3 mL HBSS-BG (HBSS with 0.1% BSA and 1% glucose) using a 22-gauge needle (Becton Dickinson, Franklin Lakes, NJ) attached to a 3-mL syringe. The cells were pelleted by centrifugation at 600*g* for 10 minutes at 4°C, and then they were resuspended in 3 mL 45% Percoll (Pharmacia, Uppsala, Sweden). Two milliliters each of the 62%, 55%, and 50% Percoll solutions were layered successively onto 3 mL 81% Percoll solution. One hundred percent Percoll stock solution was made by mixing 9 vol Percoll with 1 vol 10 × HBSS (Life Technologies, Gaithersburg, MD). Cells in 45% Percoll were layered on top of the gradient. After centrifugation at 1600*g* for 30 minutes at 10°C, the cell band between the 81% and 62% layer was collected and then washed twice in 10 mL HBSS-BG before being resuspended in 3 mL HBSS-BG. These cells were layered over 3 mL Histopaque 1119 (Sigma) and centrifuged at 1600*g* for 30 minutes at 10°C to remove contaminating red blood cells (RBCs). The cells between the Histopaque 1119 and HBSS-BG layers were harvested and washed twice in 10 mL HBSS-BG. The final cell preparation was kept on ice in 2 mL PBS (without Ca^{2+} and Mg^{2+}). Cells collected from bone marrow of mice were spun onto glass slides; confirmation of the enriched neutrophil population was checked by assessment of nuclear morphology of Diff-Quick (Dade, Miami, FL) staining.

Measurement of intracellular ROS production

Ba/F3GR and Ba/F3GRprox or 32DGR cells were resuspended in fresh medium. At 24 hours, 10^7 cells/sample were harvested, washed twice with PBS, and resuspended in 10 mL prewarmed serum-free medium without recombinant IL-3 or G-CSF for 5 hours. Samples were split equally and transferred into 14-mL Falcon polypropylene round-bottom tubes (Becton Dickinson Labware, Franklin Lakes, NJ). The 5-mL cell suspension was then loaded with 5 μL dihydrorhodamine 123 (DHR) or 10 μM 2′,7′-dichlorodihydrofluorescein diacetate (H_2DCF) (Molecular Probes, Eugene, OR) solution (final concentration 5 μM). The cells were incubated at 37°C for 20 minutes followed by stimulation with or without 100 ng/mL G-CSF for indicated time periods or variable concentrations of G-CSF for 30 minutes. Unstimulated cells were used as a control for basal level of fluorescence. Aliquots of cells were harvested at indicated time points and placed on ice to stop the reaction. Triplicate samples were analyzed on a Becton Dickinson FACScan (fluorescence-activated cell scanner) with the FL1 channel. Results were analyzed with CellQuest software (Becton Dickinson). Values of increased (by subtracting basal level of fluorescence) mean fluorescence intensity were used for statistical analysis. The 2-tailed Student *t* test was used to compare different groups.

Immunoprecipitation and immunoblotting

Cell lysis with 1% NP-40 detergent was performed as described elsewhere.[15] Protein concentration was determined using the Bradford protein assay. For immunoprecipitation, cell lysates were incubated first with rabbit anti-p47^{phox} antibody overnight at 4°C, then with 20 μL protein A/G-Sepharose (Santa Cruz Biotechnology) for 1 hour on a roller system at 4°C. The beads were washed 4 times with lysis buffer. For Western blot analysis, cell lysates or immunoprecipitates were subjected to sodium dodecyl sulfate–polyacrylamide gel electrophoresis (SDS-PAGE), and proteins were transferred onto Immobilon-P Transfer Membrane (Millipore Corporation, Bedford, MA). The membranes were blocked for 1 hour at room temperature with blocking buffer (5% milk in PBS with 0.1% Tween-20). The blots were then incubated with primary antibodies for 2 to 4 hours at room temperature, followed by incubation with secondary antibodies for 1 hour at room temperature. The immunoreactive bands were visualized by enhanced chemiluminescence (Amersham, Piscataway, NJ).

Membrane translocation of p47^{phox}

Ba/F3GR cell equivalents (10^7) were used for each sample. After the cells were washed twice with PBS, they were resuspended in serum-free medium for 5 hours. Cells were then resuspended in fresh medium and unstimulated or stimulated with 100 ng/mL G-CSF for 10 minutes at 37°C. Samples were then placed on ice and centrifuged. Then, the cells were resuspended in relaxation buffer (100 mM KCl, 3 mM NaCl, 3.5 mM $MgCl_2$, 1.25 mM EGTA, 20 μM phenylmethanesulfonyl fluoride, 80 μg/mL leupeptin, 20 μg/mL pepstatin A, 20 μg/mL chymostatin, and 10 mM HEPES, pH 7.4). The cells were lysed by 3 rounds of 5-second sonication on ice using a Branson 250 sonicator (Branson Sonic Power, Danbury, CT) set at maximum power output for a microtip. The sonicates were then centrifuged at 10 000*g* for 10 minutes. Supernatants (1 mL) were overlaid on a discontinuous sucrose gradient consisting of 2 mL 40% (wt/vol) and 1.5 mL 15% (wt/vol) sucrose cushion. This material was subjected to ultracentrifugation at 170 000*g* for 60 minutes. The cytosolic fraction consisted of the

high-speed supernatant, the membrane fraction of the layer between the 40% and 15% sucrose cushions. The cytosolic and membrane fractions were resuspended in 2 × Laemmli sample buffer, boiled for 5 minutes, and stored at −20°C. Proteins were analyzed by Western blot with the anti-p47^{phox} antibody and developed by using enhanced chemiluminescence (ECL).

Akt siRNA treatment of Ba/F3GR cells

Mouse Akt1 siRNA (Mm_Akt1_5_HP siRNA, catalog no. SI02652440, which targets the sequence at codons 725-745 AACGAGTTTGAGTACCTGAAA) and nonsilencing control siRNA (control siRNA, catalog no. 1022076) were purchased from Qiagen (Valencia, CA). Cell line nucleofector Kit V for the Ba/F3 cell line was purchased from Amaxa Biosystems (Gaithersburg, MD). Nucleofection of BaF3/GR cells was performed according to manufacturer's optimized protocol. Briefly, 2×10^6 cells per Nucleofection sample were harvested after cells were freshly split, and the cell pellet was resuspended in prewarmed Nucleofector solution V. Cell suspension (100 μL) was incubated with siRNA or control (200 nM each) and transferred into Amaxa-certified cuvettes. Nucleofection was carried out according to program X-01. Cells were harvested after 24 hours for analysis by Western blot for Akt levels and flow cytometry for ROS production.

Measurement of cell proliferation and cell-cycle analysis to G-CSF

To measure the growth of Ba/F3GR and Ba/F3GRprox cells in response to G-CSF, cells were seeded into fresh culture medium at a density of 1×10^5 cells/mL in the presence of 100 ng/mL G-CSF with or without1 mM or 10 mM NAC. Cell numbers were determined daily for 3 days after exposure to G-CSF with the use of direct count on the basis of trypan blue exclusion assay. For cell-cycle analysis, 1×10^6 cells were harvested for each sample and washed with 5 mL PBS for 1 time. Cells were resuspended in 0.9 mL PBS and 2.1 mL 100% ethanol for fixing for at least 1 hour. Before staining with propidium iodide (PI; Sigma), the cells were washed twice with PBS before being stained in 1 mL PI solution (50 μg/mL PI, 1% Triton X-100, 1 mg/mL sodium citrate, 10 μg/mL RNase in 1 × PBS) at 4°C for 1 to 2 hours. Flow cytometric analysis was performed, and the data were analyzed by Modfit LT software (Verity Software House, Topsham, ME).

Results

G-CSF induction of ROSs

G-CSF is essential for the production of neutrophils and is a critical mediator for enhancing nonspecific host resistance to bacterial infection.[32] G-CSF has also been shown to increase cellular oxidative stress, but the mechanism has not been identified. To assess whether G-CSF directly induces the production of intracellular ROSs, Ba/F3GR cells were treated with variable concentrations of G-CSF or for variable time periods. G-CSF–induced intracellular ROS production was measured by flow cytometry using oxidant-sensitive probe DHR123 (DHR), which is a cell-permeable, nonfluorescent molecule. On interaction with free radicals, DHR is oxidized, resulting in the liberation of rhodamine123, a highly fluorescent marker. The relative intracellular ROS level induced by G-CSF was determined by monitoring the relative fluorescence of rhodamine123 in the cells. The increased mean fluorescence (mean ± SD) induced by G-CSF was calculated by subtraction from unstimulated samples. A G-CSF dose-dependent increase of intracellular ROS production was detected in Ba/F3GR cells (Figure 1A). We next determined the kinetics of G-CSF–stimulated intracellular ROS production. G-CSF–stimulated production of intracellular ROSs became detectable as early as 1 minute in Ba/F3GR cells and peaked at 30 minutes in response to G-CSF (Figure 1B). Similar results were obtained when cells were analyzed with H_2DCF, another fluorogenic reagent that detects ROSs (data not shown).

To confirm the direct role of G-CSF in the production of ROS, we established stable transfectants of the full-length G-CSF receptor in another myeloid cell line, 32D. Comparable levels of

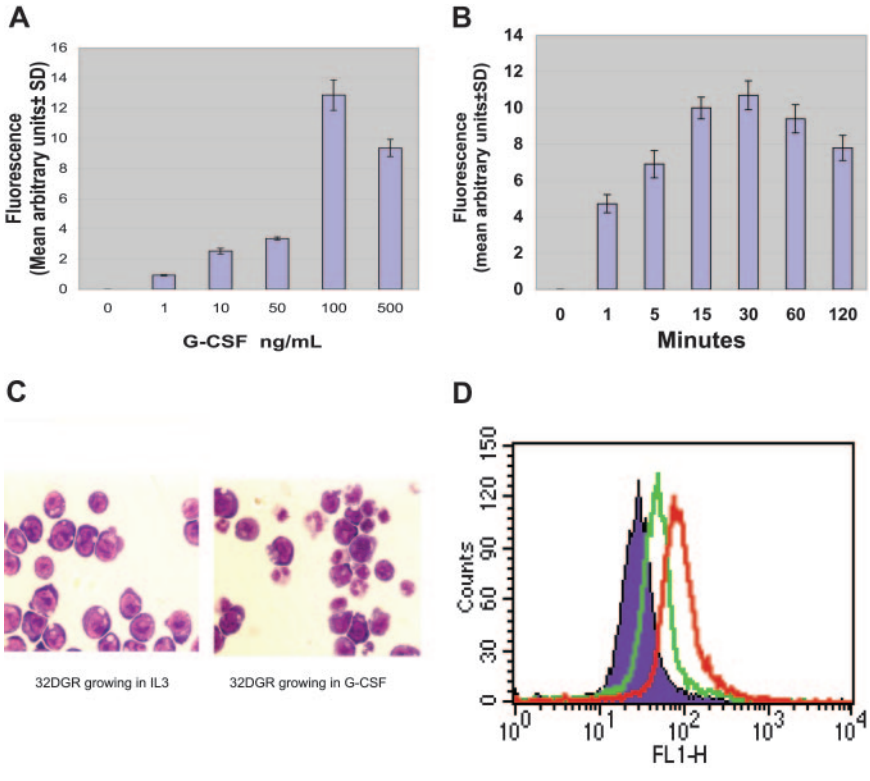

Figure 1. G-CSF–induced intracellular ROS production. Ba/F3 cells stably transfected with the wild-type G-CSF receptor were treated with variable G-CSF concentrations or for variable time periods. ROS production was measured in cells labeled with DHR. ROS levels induced by G-CSF normalized to that of untreated cells were determined by monitoring the increased fluorescence in the cells. (A) Dose-dependent increase in intracellular ROS production (mean ± SD). (B) Time course for increased intracellular ROS production (mean ± SD). (C) G-CSF–induced neutrophil differentiation. (Left) 32DGR cells grown in medium with IL-3 appear as myeloblasts. (Right) 32GR cells grown in medium with 100 ng/mL G-CSF for 10 days display a population of granulocytes (Giemsa staining; × 200 magnification). Photographs were obtained using a Nikon Microphot-FX microscope (Nikon, Tokyo, Japan) and a Nikon plan/apo 20×/0.75 numeric aperture objective lens. Images were captured using a Sony 3CCD color video camera, model DXC-990 (Sony, Tokyo, Japan) and were processed using Acquisitions software (Media Cybernetics, Silver Spring, MD). (D) G-CSF–induced intracellular ROS production in 32DGR cells. Purple indicates unstimulated cells; green, G-CSF for 30 minutes; red, 100 μM H_2O_2 for 30 minutes.

human G-CSF receptors were expressed in 32D, as detected by flow cytometry and Western blot assay (data not shown). Cells that did not express the G-CSF receptor did not survive after 48 hours in G-CSF medium, whereas the 32D cells expressing G-CSF receptor survived in G-CSF medium for more than 1 week and differentiated into granulocytes (Figure 1C). We measured G-CSF–induced intracellular ROS production in 32DGR cells. Cells were loaded with 5 μM DHR123 for 20 minutes followed by either no or 100 ng/mL G-CSF or 100 μM H_2O_2 (as a positive control) for 30 minutes. G-CSF treatment of 32DGR cells also resulted in ROS production (Figure 1D).

Activation of Lyn, Akt, and ERK1/2 by G-CSF

Because previous studies have suggested a role for Src in ROS production,[33-35] we assayed for the phosphorylation status of activated Lyn by Western blotting for phosphorylated Lyn Y396 (the positive regulatory phosphorylation site) and Lyn Y507 (the negative regulatory phosphorylation site). The commercially available antibody, which was developed against the phosphorylated Src Y416 residue, will recognize the highly conserved tyrosine phosphorylation site (EDNEpYTAR) in other members of the Src kinase family. The corresponding tyrosine site in Lyn is position 396 and is recognized by the anti–phosphor-Src Y416 antibody. Lyn is the predominant Src kinase in Ba/F3, although smaller amounts of Hck and Fyn may be found (data not shown). After engagement of the wild-type G-CSF receptor, Lyn activation increased as demonstrated by the phosphorylation of LynY396 and the dephosphorylation of Lyn Y507. Lyn activation occurred as rapidly as 1 minute, peaking at 5 minutes, and diminishing after 15 minutes (Figure 2A). Because there is an increase in the tyrosine phosphorylation of Lyn at its negative regulatory site (ie, Tyr507) before 60 minutes, Lyn's kinase activity is transient in cells expressing full-length receptor. We next examined the kinetics of G-CSF–induced phosphorylation of Akt, a surrogate marker for PI3-kinase activity. G-CSF–induced serine phosphorylation of Akt occurred at 1 minute, peaked at 5 minutes, declined to near basal levels after 15 minutes in Ba/F3GR cells (Figure 2B). We also examined the kinetics of G-CSF–induced activation of the ERK. Phosphorylation of ERK1/2 Thr202/Tyr204 was observed with 1 minute of stimulation, peaked at 5 minutes, diminished after 15 minutes in Ba/F3GR (Figure 2C). These results suggest that G-CSF induces the activation of Lyn, Akt, and ERK1/2 with a similar time course.

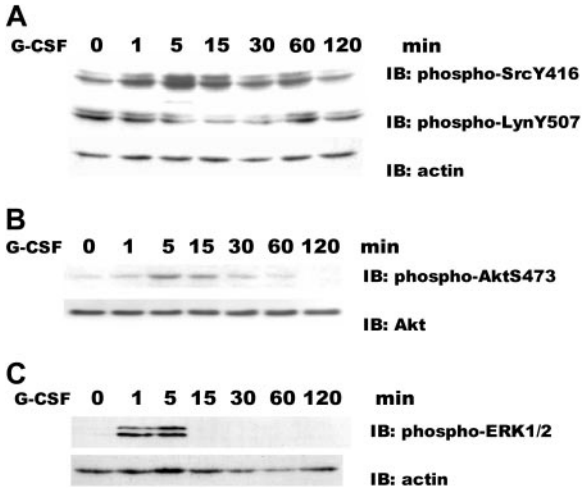

Figure 2. Time course for G-CSF–induced activation of Lyn, Akt, and ERK1/2. Ba/F3GR cells were stimulated with or without 100 ng/mL G-CSF for indicated time periods, then whole-cell lysates were prepared. (A) Lyn activation. Immunoblotting (IB) was performed using anti–phospho-Src Y416 antibody, which detects the activated state of Lyn, and anti–phospho-Lyn Y507, which detects the nonactivated state of Lyn. The blot was stripped and reprobed with antiactin antibody to demonstrate comparable levels of protein loaded in respective lanes. (B) Akt activation. Immunoblotting was performed using anti–phospho-Akt S473 antibody and reprobed with anti-Akt antibody. (C) ERK1/2 activation. Immunoblotting was performed using anti–phospho-ERK1/2 2T202/Y204 antibody and reprobed with antiactin antibody. Comparable results were observed in 4 independent experiments.

Small molecule inhibition of G-CSF–induced Akt or ERK1/2 activation

Lyn has been reported to be upstream of Akt[17] and ERK1/2[21] in intracellular signaling cascades. Akt[26] and ERK1/2 have been shown to phosphorylate $p47^{phox}$ and are therefore likely mediators for G-CSFR–induced ROS production. Pharmacologic inhibitors of Akt and MEK were used to analyze the effect on the phosphorylation of Akt and ERK1/2 in ROS production. We first investigated the effect of A838450, a specific Akt inhibitor, on the phosphorylation of mTOR and GSK3, downstream substrates of Akt. G-CSF–induced phosphorylation of mTOR and GSK3 was blocked in Ba/F3GR cells pretreated for 1 hour with the Akt inhibitor A838450 in a dosage-dependent manner (Figure 3A), these data indicated Akt kinase activity is inhibited by A838450. We next determined the effect of A838450 on the phosphorylation of Akt, and MEKI, an ERK1/2 inhibitor, on the activation of ERK1/2. Ba/F3GR cells were pretreated for 1 hour with the indicated concentrations of Akt inhibitor A838450, the MEK inhibitor, or DMSO (the diluent control) and followed by stimulation with or without 100 ng/mL G-CSF for 10 minutes. Treatment of Ba/F3GR cells with A838450 caused a dosage-dependent inhibition of Akt phosphorylation ($IC_{50} \sim 1$ μM), but phosphorylation of ERK1/2 was unaffected (Figure 3B). Treatment of Ba/F3GR cells with MEK inhibitor caused a dosage-dependent inhibition of ERK1/2 phosphorylation ($IC_{50} \sim 1$ μM), whereas phosphorylation of Akt was unaffected (Figure 3C). These results demonstrate that these 2 kinase inhibitors specifically inhibit the kinase activity of Akt or ERK1/2.

Correlation of kinase inhibitors and Lyn abrogation with suppression of ROSs

To address the signaling pathways leading to ROS production and to evaluate whether G-CSF–induced ROS production is Lyn-PI3-kinase-Akt dependent, we used pharmacologic inhibitors of these signaling molecules. Ba/F3GR cell lines were treated with PP1 (Src inhibitor), Ly294002 (PI3-kinase inhibitor), A838450 (Akt inhibitor), and MEKI for 60 minutes before being stimulated with G-CSF. The results show that G-CSF–induced production of ROSs was significantly decreased by pretreatment with Src kinase inhibitor PP1, PI3-kinase inhibitor Ly294002, and Akt inhibitor A838450 (Figure 4A-B). In contrast, the MEK inhibitor did not affect G-CSF–induced production of ROSs. To confirm a role for Akt in promoting ROS production, we treated Ba/F3GR cells with siRNA to Akt. ROS production was significantly reduced in cells treated with Akt siRNA when compared with scrambled siRNA (Figure 4C). To further address Lyn's role in G-CSFR–mediated ROS production, flow cytometry to detect ROS production was performed on bone marrow–derived neutrophils from wild-type and $Lyn^{-/-}$ mice (Figure 4D). Compared with wild type, G-CSF–induced ROS production was significantly reduced in neutrophils from Lyn-deficient mice (Figure 4E). These data suggest that

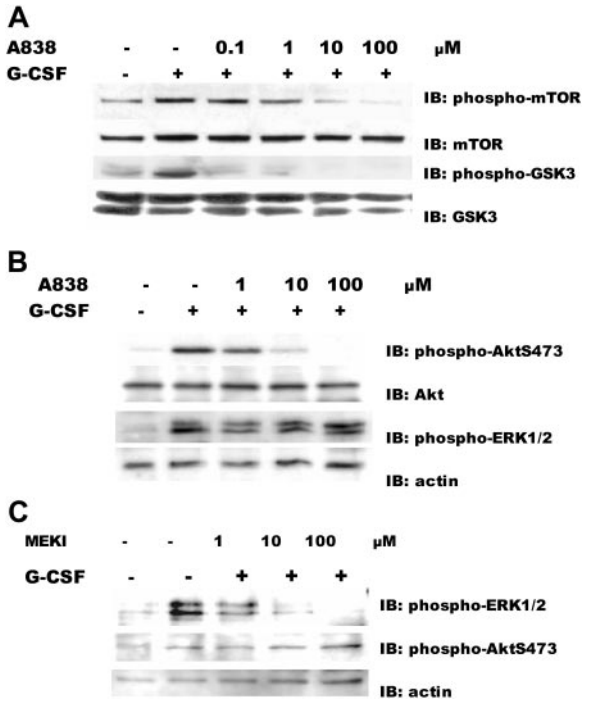

Figure 3. Effect of kinase inhibitors on G-CSF–induced activation of Akt or ERK1/2. (A) Inhibition of downstream substrates of Akt, mTOR, and GSK3 by a specific Akt inhibitor A838450. Ba/F3GR cells were pretreated for 1 hour with the indicated concentrations of Akt inhibitor A838450 or DMSO (the diluent control), then stimulated with or without 100 ng/mL G-CSF. Lysates were prepared, and immunoblotting was performed using anti–phospho-mTOR S2448 or anti–phospho-GSK3 S21/9 antibodies. Blots were stripped and reprobed with anti-mTOR or anti-GSK3 antibody to demonstrate comparable protein loading. (B) Akt inhibition. Ba/F3GR cells were pretreated for 1 hour with the indicated concentrations of Akt inhibitor A838450 or DMSO (the diluent control), then left unstimulated or stimulated with 100 ng/mL G-CSF. Lysates were prepared, and immunoblotting was performed using anti–phospho-AktS473 and anti–phospho-ERK1/2 T202/Y204 antibody. Blot was stripped and reprobed with anti-Akt or antiactin antibody to demonstrate comparable protein loading. (C) ERK1/2 inhibition. Ba/F3GR cells were pretreated with the indicated concentrations of MEK inhibitor or DMSO (diluent control) for 1 hour and then stimulated with 100 ng/mL G-CSF. Lysates were prepared, and immunoblotting was performed using anti–phospho-ERK1/2 T202/Y204 antibody or anti–phospho-Akt S473. Blot was stripped and reprobed with antiactin antibody to demonstrate comparable protein loading.

G-CSF–induced production of ROS requires activation Lyn-PI3-kinase-Akt pathway, not Erk1/2.

G-CSF activation of NADPH oxidase component, p47^{phox}

A major source of ROSs in blood cells, NADPH oxidase requires the serine phosphorylation of p47^{phox} for its activation. Several serine kinases, such as Akt and ERK1/2, have been suggested to phosphorylate p47^{phox}. Because G-CSF activates both Akt and ERK1/2,[17,21-23,36,37] we hypothesized that G-CSF could lead directly to NADPH oxidase activation through either serine kinase. We suspected that Akt was the principle mediator based on the small molecule inhibitor data. We found that G-CSF stimulation resulted in prompt phosphorylation of p47^{phox} in a time-dependent manner (Figure 5A), whereas the PI3-kinase and Akt inhibitors inhibited the serine phosphorylation of p47^{phox} (Figure 5B). To further demonstrate that G-CSF activates NADPH oxidase, in part through the serine phosphorylation of p47^{phox}, we determined whether G-CSF induced its translocation to the plasma membrane. We recovered the membrane fraction by centrifugation through a discontinuous sucrose gradient followed by SDS-PAGE and immunoblotting with specific anti-p47^{phox} antibody. Under basal conditions, p47^{phox} was present at higher levels in the cytosol than in the membrane (Figure 5C, lane 4 from cytosolic fraction and lane 6 from membrane fraction). After G-CSF stimulation, p47^{phox} content was reduced in the cytoplasmic fraction but increased in the membrane fraction (Figure 5C, lane 5 from cytosolic fraction and lane 7 from membrane fraction). Because we found that the kinetics of Akt and ERK1/2 activation were similar (Figure 2B-C), we reasoned that there should be a temporal correlation of serine phosphorylation of p47^{phox} to that of either Akt or ERK1/2. To determine which serine kinase might be responsible for G-CSF–induced phosphorylation of p47^{phox}, we analyzed the effects of kinase inhibitor on the membrane translocation of p47^{phox}. Pretreatment with the Akt inhibitor impaired membrane translocation of p47^{phox} following G-CSF stimulation, whereas the MEK inhibitor had no effect (Figure 5D). To determine whether NADPH oxidase is involved in G-CSF receptor–mediated ROS production, we incubated cells with DPI, a specific inhibitor of NADPH oxidase.[38] Pretreatment with 0.1 μM DPI reduced or 1 μM DPI blocked G-CSF–induced intracellular ROS production (Figure 5E). These data support our finding that G-CSF induced ROS production via NADPH oxidase and the phosphorylation of p47^{phox} by Akt, not Erk1/2.

Truncated G-CSF receptor increases ROS production

Almost all of the children who develop acute myeloid leukemia following G-CSF treatment of their severe congenital neutropenia possess an acquired nonsense mutation of the receptor. Whether this mutation is leukemogenic is uncertain, but its expression leads to hyperproliferation without differentiation of expressing cells. To determine whether a truncated G-CSF receptor contributes to ROS production, we studied Ba/F3 cells stably expressing truncated receptor. Flow cytometry and Western blotting documented comparable levels of surface receptor expression as reported previously.[17] As shown in Figure 6A, ROS production was detected as rapidly as 1 minute after G-CSF stimulation, peaked at 30 minutes, and returned to baseline by 60 minutes in cells expressing full-length receptor. In contrast, in Ba/F3GRprox cells, the basal level of ROS was higher that that of Ba/F3GR, and G-CSF–induced ROS production persisted for 120 minutes. The higher basal level of ROS production in Ba/F3GRprox may be due in part to elevated basal activity of Lyn.

The most commonly found mutation in patients with severe congenital neutropenia and acute myeloid leukemia (AML), the nonsense mutation resulting in a truncated G-CSF receptor at codon 715 was genetically engineered in mice. Bone marrow neutrophils showed hyperresponsiveness to G-CSF. To demonstrate that the stimulation of the truncated G-CSF receptor results in enhanced ROS production, neutrophils from bone marrow of wild-type and GRΔ715 mice were purified, and G-CSF–induced ROS production was measured by flow cytometry. ROS production was significantly higher in neutrophils expressing the truncated receptor than the full-length (Figure 6B). We next correlated the increased ROS production with the activation status of Lyn, Akt, and ERK1/2 following G-CSF stimulation. Compared with cells expressing full-length receptor, there was prolonged phosphorylation of Tyr396 of Lyn, which reflects the activation state of Lyn in cells with the truncated receptor (Figure 6C). Prolonged and enhanced Akt phosphorylation was also observed in Ba/F3GRprox cells (Figure 6D). However, the phosphorylation of ERK1/2 Thr202/Tyr204 was observed within 1 minute of stimulation, peaked at 5 minutes, and declined after 15 minutes (Figure 6E). This time course of ERK1/2 activation did not correlate with ROS production. These data demonstrate that G-CSF stimulation of cell

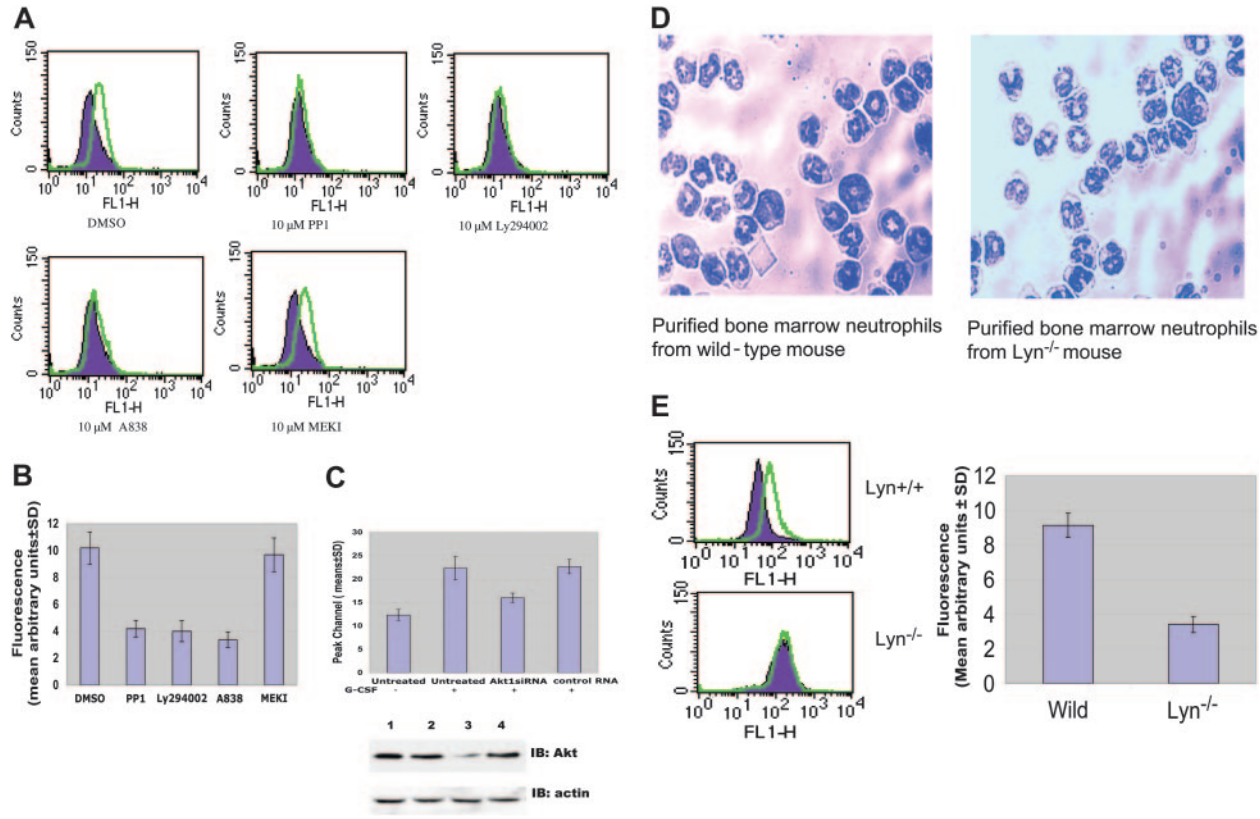

Figure 4. Inhibition of G-CSF–induced intracellular ROS production. Ba/F3GR cells were pretreated with the Src kinase inhibitor PP1, PI3-kinase inhibitor LY294002, Akt inhibitor A838450, or ERK1/2 inhibitor MEKI for 1 hour and then stimulated with 100 ng/mL G-CSF for 30 minutes (green) or not (purple). The increased levels of intracellular ROSs were determined by flow cytometry. (A) Inhibition of ROS production by kinase inhibitors. Results from a representative experiment. (B) Effects of kinase inhibitors on ROS production due to G-CSF (mean ± SD). (C) Effect of siRNA knock-down of Akt on ROS production. Ba/F3GR cells were treated for 24 hours with 200 nM siRNA to murine Akt1, scrambled sequence, or mock nucleofection. Cell lysates were analyzed for Akt and actin protein expression. Cells were also stimulated with 100 ng/mL G-CSF for 60 minutes or not, stained with DHR, and then analyzed for ROS production by flow cytometry. Data represented the mean ± SD. (Bottom) Western blot of nucleofected Ba/F3GR cells. Lane 1, untransfected cells; lane 2, mock nucleofection of cells; lane 3, nucleofection with Akt1 siRNA; lane 4, scrambled siRNA. (D) Neutrophils from bone marrow of wild-type and *Lyn*$^{-/-}$ mice. The results showed that more than 95% of cells are neutrophils. Images obtained as in Figure 1C. (E) G-CSF–induced ROS production was impaired in neutrophils from *Lyn*$^{-/-}$ mice. Neutrophils from bone marrow of wild-type and Lyn$^{-/-}$ mice were loaded with 5 μM DHR with (green) or without (purple) 100 ng/mL G-CSF for 60 minutes. One representative is shown in the left panel; quantitative results (mean ± SD) were shown in the right panel.

lines and neutrophils expressing a truncated G-CSF receptor resulted in greater levels of ROSs. These results imply that higher levels of ROSs may contribute G-CSF hyperresponsiveness found in these cells.

Antioxidant *N*-acetyl-L-cysteine reduced the ROS production and cell proliferation by inhibiting Akt activation

NAC, a thiol-containing radical scavenger and glutathione precursor, is capable of enhancing the toxicity of other chemicals that exert anticancer activity via different mechanisms. Because NAC is believed to combat cancer via different mechanisms, we sought to determine whether NAC inhibits the activation of Akt and reduces the ROS production in Ba/F3GR and Ba/F3GRprox cells. Ba/F3GR and Ba/F3GRprox cells were treated with or without 1 mM or 10 mM NAC, respectively, for 60 minutes followed by measuring phosphorylation of Akt, ERK1/2, or p38, and intracellular ROS production in the absence or presence of G-CSF. G-CSF–induced Akt phosphorylation was inhibited by NAC treatment (Figure 7A top), whereas phosphorylation of ERK1/2 and p38 were not inhibited by NAC treatment by reblotting with phospho-ERK1/2 (Figure 7A bottom) or phospho-p38 antibody (data not shown). G-CSF–induced ROS production was diminished by the administration of NAC (Figure 7B). To investigate the effect of a change in oxidative status on cell proliferation, Ba/F3GR and Ba/F3GRprox cells were exposed to 0, 1 mM, or 10 mM NAC for 24, 48, and 72 hours in the presence of G-CSF. As shown in Figure 7C, NAC inhibited cell proliferation in a dose-dependent manner. To further address the effect of NAC on the cell-cycle progression and survival, Ba/F3GR and Ba/F3GRprox cells were treated with 10 mM NAC for 48 hours in the presence of 100 ng/mL G-CSF followed by cell-cycle analysis. As shown in Figure 7D and Table 1, the fraction of cells in S phase decreased, whereas those in G_1 phase increased when cells were treated with 10 mM NAC. These data indicated that NAC reduced cell proliferation without cytotoxicity. When added to Ba/F3GR cells, H_2O_2 resulted in a biologic dose-dependent growth. Although high dose (100 μM) resulted in cell death, lower doses (0.1-10 μM) enhanced cell growth (Figure 7E). Together, these findings suggest that enhanced G-CSF–induced ROS production in cells expressing a truncated receptor contributes to cell proliferation and suggest that the use of an antioxidant might inhibit leukemogenesis through the attenuation of oxidative stress, particularly in patients with aberrant G-CSF receptors or signaling.

Discussion

Because a variety of inflammatory cytokines induces a rapid increase of intracellular ROSs, we investigated the ability of

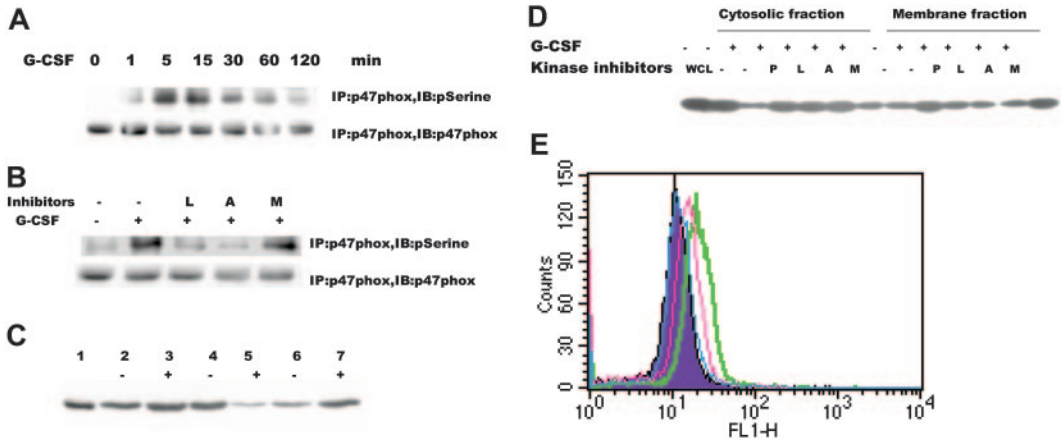

Figure 5. G-CSF induced activation of p47^{phox}. (A) Serine phosphorylation of p47^{phox} induced by G-CSF. Ba/F3GR cells were treated with or without 100 ng/mL G-CSF for indicated time periods, and lysates were prepared. Proteins were immunoprecipitated with anti-p47^{phox} antibody and blotted with either anti-phosphoserine antibody or anti-p47^{phox} antibody. The latter demonstrates comparable protein loading. (B) Inhibition of serine phosphorylation of p47^{phox} by kinase inhibitors. Ba/F3GR cells were untreated or pretreated with kinase inhibitors for 1 hour, followed by no or 100 ng/mL G-CSF for 60 minutes, then the lysates were prepared. Proteins were immunoprecipitated with anti-p47^{phox} antibody and blotted with either anti-phosphoserine antibody or anti-p47^{phox} antibody. (C) Membrane translocation of p47^{phox}. Ba/F3GR cells were untreated or treated with 100 ng/mL G-CSF for 10 minutes, and then cells were lysed and subjected to ultracentrifugation. Membrane and cytosolic fractions were purified and then subjected to electrophoresis and immunoblotting with anti-p47^{phox} antibody. Lane 1, whole-cell lysate from Ba/F3GR cells; lanes 2-3, whole-cell lysates after sonication; lane 4, cytosolic fraction of Ba/F3GR cells unstimulated by G-CSF; lane 5, cytosolic fraction of Ba/F3GR cells stimulated by G-CSF; lane 6, membrane fraction of Ba/F3GR cells unstimulated by G-CSF; lane 7, membrane fraction of Ba/F3GR cells stimulated by G-CSF. (D) Abrogation of membrane translocation of p47^{phox} following treatment with Src or Akt kinase inhibitors. Ba/F3GR cells were pretreated with DMSO (−) or Src kinase inhibitor PP1 (P), the PI3K inhibitor Ly294 002 (L), the Akt inhibitor A838450 (A), or ERK1/2 inhibitor MEKI (M) for 1 hour, followed by stimulation with 100 ng/mL G-CSF for 10 minutes. Cytosolic and membrane fractions were prepared and analyzed for trafficking of p47^{phox}. Comparable results were obtained in 3 independent experiments. (E) DPI, a specific inhibitor of NADPH oxidase, blocked G-CSF–induced ROS production. Ba/F3GR cells were pretreated with 0.1 μM or 1 μM DPI for 1 hour, loaded with 5 μM DHR for 10 minutes, and then stimulated with 100 ng/mL G-CSF for 30 minutes. ROS production was determined by flow cytometry. Purple indicates untreated cells without G-CSF; green, untreated cells + G-CSF; pink, 0.1 μM DPI + G-CSF; blue, 1 μM of DPI + G-CSF.

G-CSF, the most critical growth factor for neutrophil production, to affect ROSs. Here, we show that G-CSF induced ROS production in both a time-dependent and dose-dependent fashion in G-CSF receptor–transfected murine Ba/F3 cells and 32D cells. Because NADPH oxidase is a major generator of ROSs in blood cells, we showed that G-CSF–induced ROS production was dependent on NADPH oxidase and determined that G-CSF promoted its assembly. Phosphorylation of p47^{phox} results in its recruitment to the membrane, and this event may result from the activity of a serine kinase, such as ERK1/2 or Akt. Because G-CSF causes the

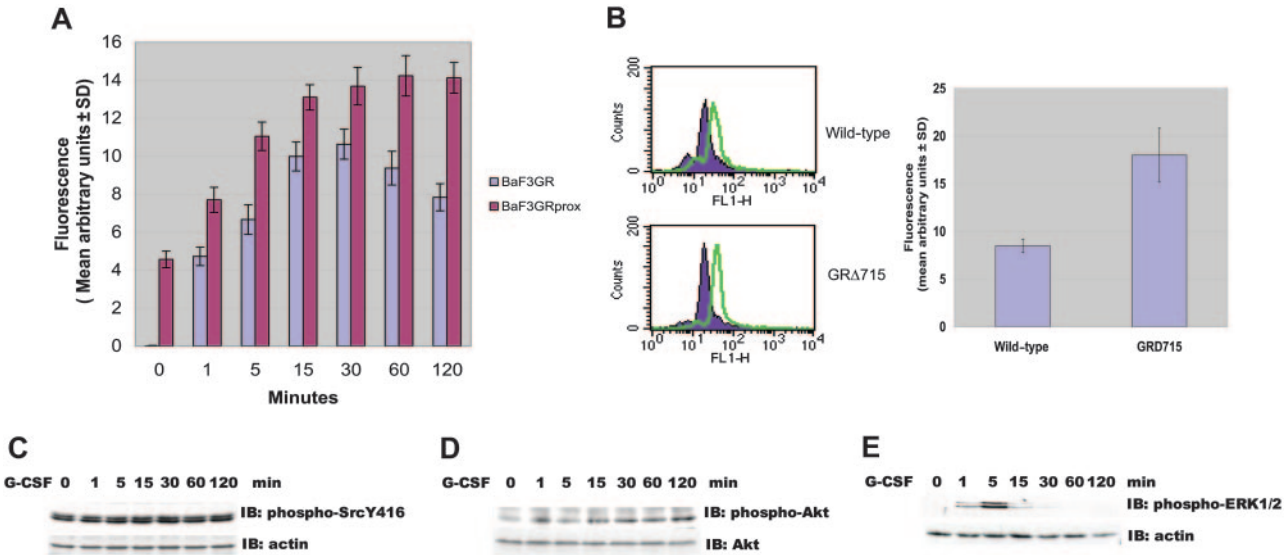

Figure 6. Enhanced ROS production in cells expressing a truncated G-CSF receptor. (A) Increased ROS production in cells expressing the truncated G-CSF receptor. Stable transfectants of Ba/F3 cells, expressing comparable levels of either wild-type or truncated G-CSF receptor, were labeled with dihydrorhodamine123 and unstimulated or stimulated with 100 ng/mL G-CSF for indicated periods of time. The relative ROS level induced by G-CSF was determined by monitoring the increased fluorescence (means ± SD) of rhodamine123 in the cells. (B) Truncated G-CSF receptor knock-in mice showed enhanced ROS production. Neutrophils from bone marrow of wild-type and GRΔ715 mice were loaded with DHR followed by stimulation with 100 ng/mL G-CSF for 60 minutes (green) or not (purple). One representative is shown in the left panel; quantitative results (means ± SD of 3 independent experiments) are shown in the right panel. (C) G-CSF–induced sustained activation of Lyn in Ba/F3GRprox. Immunoblotting was performed using anti–phospho-Src Y416 antibody, which detects the activated state of Lyn. Blot was stripped and reprobed with antiactin antibody to demonstrate comparable levels of protein loaded in respective lanes. (D) G-CSF–induced activation of Akt in Ba/F3GRprox. Immunoblotting was performed using anti–phospho-Akt S473 antibody, then the blot was stripped and reprobed with anti-Akt antibody to demonstrate comparable levels of protein loaded in respective lanes. (E) G-CSF–induced activation of ERK1/2 in Ba/F3GRprox. Immunoblotting was performed using anti–phospho-ERK1/2 T202T204 antibody, then the blot was stripped and reprobed with antiactin antibody to demonstrate comparable levels of protein loaded in respective lanes.

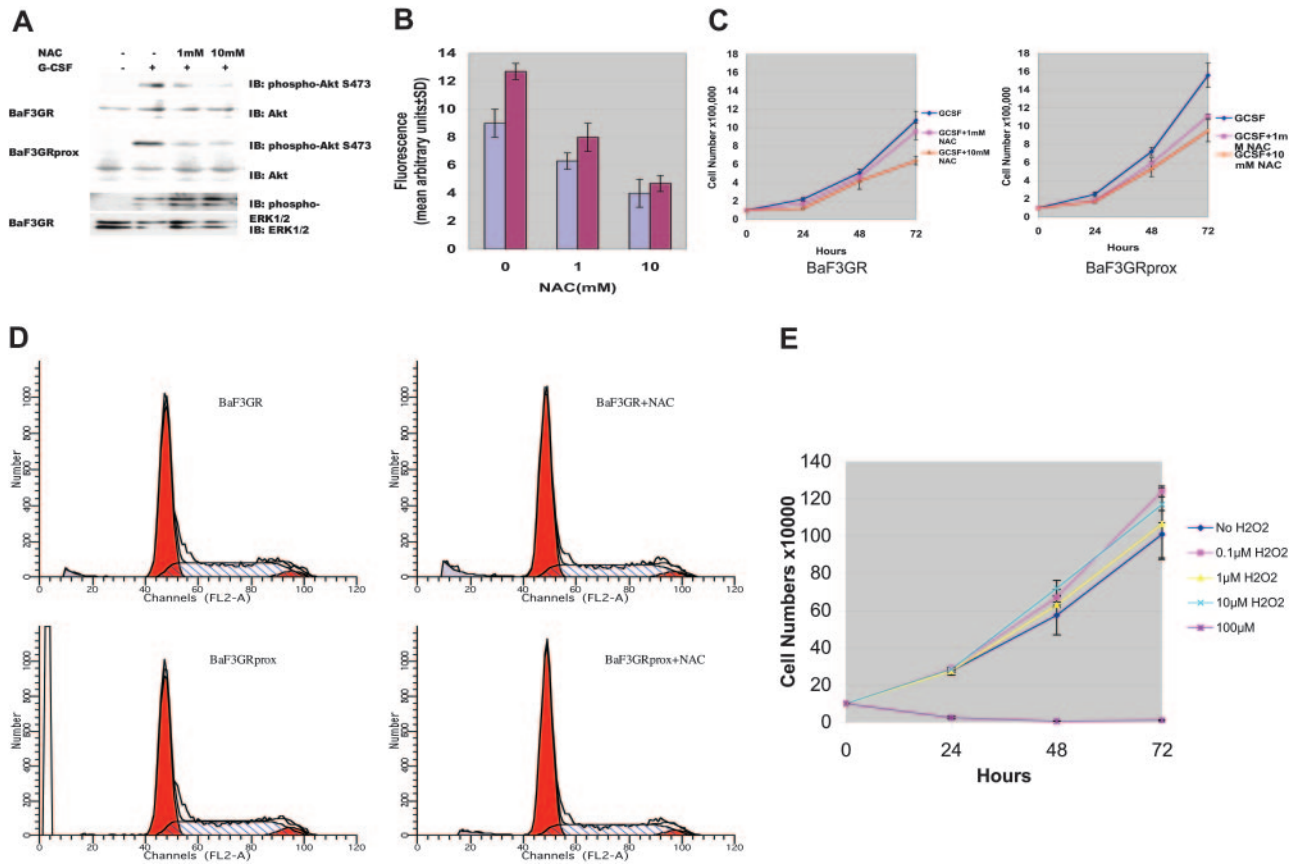

Figure 7. *N*-acetyl-L-cysteine on the ROS production and cell proliferation. (A) Effect of NAC on the activation of Akt and ERK1/2. Ba/F3GR and Ba/F3GRprox cells were pretreated without or with 1 mM or 10 mM NAC, respectively, for 1 hour, followed by stimulation with or without100 ng/mL G-CSF for 10 minutes. Cell lysates were prepared and blotted with anti–phosphor-Akt S473 or anti–phospho-ERK1/2 antibody and reprobed with Akt or ERK1 antibody. (B) G-CSF–induced ROS production was diminished by the administration of NAC. Ba/F3GR and Ba/F3GRprox cells were pretreated with or without1 mM or 10 mM NAC, respectively, for 1 hour, then loaded with 5 μM DHR123 and stimulated with or without 100 ng/mL G-CSF for 30 minutes. The relative ROS level induced by G-CSF was determined by monitoring the increased fluorescence in the cells (mean ± SD). Blue bars indicate BaF3GR; red bars, BaF3GRprox. (C) NAC inhibited the proliferation of Ba/F3GR and GRprox. Ba/F3GR and Ba/F3GRprox cells growing in IL-3 were washed extensively with PBS, 10^5/mL cells for each sample was plated in G-CSF containing medium, the cells were untreated or treated with 1 mM or 10 mM NAC, and the cells were counted at 0, 24, 48, and 72 hours by trypan blue exclusive assay. The results represent 3 independent experiments. (D) Effect of NAC on cell-cycle progression. Ba/F3GR and Ba/F3GRprox cells were treated with 10 mM NAC for 48 hours in the presence of 100 ng/mL G-CSF. The cells were subjected to cell-cycle analysis by flow cytometry (Modfit LT). (E) Effect of H_2O_2 on cell growth. Trypan blue counting of Ba/F3GR cells grown in IL-3 containing medium wit or without varying doses of H_2O_2 was performed daily.

activation of both kinases, we used specific small molecule inhibitors to demonstrate that both the serine phosphorylation of $p47^{phox}$ and its translocation to the membrane was dependent on Akt. Through the use of Src family kinase inhibitor and Lyn-deficient mice, we showed that both Akt phosphorylation and ROS generation because of G-CSF were dependent on Lyn.

Previous studies demonstrated that Lyn is a redox-sensitive downstream target of NADPH oxidase and Lyn is phosphorylated by superoxide, which in turn activates SHIP (SH2-containing inositol phosphatase). This lipid phosphatase inactivates Akt by degrading the upstream phosphoinositides, thereby turning off its antiapoptotic functions, including inactivation of caspase-9 and Bad (a proapoptotic Bcl-2 family member) by phosphorylation.[18]

Table 1. Effect of NAC on cell-cycle progression (percent in each phase)

	Sub G_1, %	G_0/G_1, %	S, %	G_2/M, %
Ba/F3GR	3.72 ± 1.27	55.85 ± 0.56	40.29 ± 0.77	3.91 ± 0.72
Ba/F3GR + NAC	7.45 ± 0.27	64.01 ± 1.93	30.85 ± 1.97	5.16 ± 0.49
Ba/F3GRprox	3.85 ± 0.86	53.21 ± 0.76	41.24 ± 0.34	5.02 ± 1.09
Ba/F3GRprox + NAC	6.65 ± 1.42	61.71 ± 0.34	33.06 ± 1.63	5.23 ± 1.32

Values given are mean ± SD.

However, Lyn has numerous potential substrates, including those that lead to Akt activation.[38] In these cases, survival signals would predominate. Our data together with those reported by others in osteoclasts, leukocytes, eosinophils, macrophages, and human vascular smooth muscle cells clearly demonstrated that Lyn is upstream of NADPH oxidase. G-CSF activates Lyn, which triggers multiple signaling pathways, one of which leads to ROS production. Therefore, we postulate that a positive feed-forward loop exists whereby ROS promotes the activity of Lyn, which in turn leads to activation of PI3-kinase, Akt, and subsequent NADPH oxidase, generating more ROSs. PI3-kinase may also represent a feed-forward loop for ROS generation. In that case, ROS inactivates PTEN,[39] a critical negative regulator of 3-OH-phosphoinositides, which promotes more ROS production. Thus, the presence of 2 feed-forward loops (Lyn→PI3-kinase→Akt→$p47^{phox}$→NADPH oxidase and ROS→PTEN inactivation→increased PI3-kinase activity) favor ROS production. Other kinases, such as p38, may contribute to ROS production.[28] However, G-CSF–induced phosphorylation of p38 only in cells expressing full-length, not truncated, receptor (data not shown). Enhanced ROS production in cells expressing the truncated receptor stems from increased Lyn/PI3-kinase/Akt activation.[17] The increased activities of Lyn

and PI3-kinase are partially due to loss of negative regulation of Lyn and PI3-kinase via Shp-1 and SHIP-1.[37,40]

A few papers have reported that G-CSF did not promote ROS production in neutrophils.[41,42] Because neutrophils display more G-CSF receptors than immature cells, ROS production may be more tightly regulated in the terminally differentiated neutrophil. For instance in neutrophils, phosphatases, phospholipases, or membrane remodeling[43] may modulate G-CSF–induced serine phosphorylation or membrane translocation of p47phox. G-CSF will prime the neutrophil for enhanced ROS production following a more potent stimulus, such as f-MLP.[44] Because ROSs can be toxic to the cell, we hypothesized that excessive generation of ROSs through prolonged G-CSF signaling might be pathogenic. Prolonged G-CSF signaling occurs when the receptor is truncated as is found in patients with severe congenital neutropenia that progress to myelodysplastic syndrome (MDS) or AML.[37,40,45,46] These patients are treated with chronic pharmacologic doses of G-CSF, which augments the already abnormal G-CSF signaling. Here, we showed that when compared with cells expressing full-length G-CSF receptor, cells lines or mice genetically engineered with a truncated G-CSF receptor produced more ROSs following G-CSF stimulation. This enhanced ROS production was associated with hyperactivation of the Src kinase Lyn and Akt. In BCR/ABL$^+$ cells, ROS amplifies oncogenic tyrosine kinase signaling, contributing to transformation.[3,47] Consistent with our data, Kim et al[47] found that cells expressing the Tyr177Phe mutant of BCR/ABL failed to increase ROS production. This mutation fails to recruit the adaptor Gab2, resulting in decreased PI3-kinase activity in BCR-ABL$^+$ cells.[48]

We hypothesize that the truncated G-CSF receptor found in G-CSF–treated patients with severe congenital neutropenia who develop MDS/AML leads to a variety of sustained signaling pathways, one of which results in the excessive ROS production. Enhanced ROS production could promote cell proliferation and DNA damage, disturbances that might induce MDS/AML. Antioxidant intervention might be chemopreventive in these high-risk patients. We showed that treatment of cells expressing a truncated G-CSF receptor with an antioxidant, NAC, did reduce Akt phosphorylation, ROS generation, and cell proliferation. The truncated G-CSF receptor occurs as a somatic mutation in patients with severe congenital neutropenia and predates their progression to MDS/AML. We hypothesize that enhanced ROS production is one mechanism by which MDS/AML arises in patients with a truncated G-CSF receptor. These findings provide new insights into the G-CSF receptor signaling network proximal to NADPH oxidase in hematopoietic cells and suggest that one of the beneficial effects of therapeutic targeting of Lyn/PI3-kinase is to block ROS production and its effects on growth.

Acknowledgments

We thank Drs. Yuichiro Suzuki and Regina Day for their comments. We thank Keith Woods for chemistry support of the Akt inhibitor.

References

1. Lieschke GJ, Grail D, Hodgson G, et al. Mice lacking granulocyte colony-stimulating factor have chronic neutropenia, granulocyte and macrophage progenitor cell deficiency, and impaired neutrophil mobilization. Blood. 1994;84:1737-1746.
2. Liu F, Poursine-Laurent J, Link DC. The granulocyte colony-stimulating factor receptor is required for the mobilization of murine hematopoietic progenitors into peripheral blood by cyclophosphamide or interleukin-8 but not flt-3 ligand. Blood. 1997;90:2522-2528.
3. Sattler M, Verma S, Shrikhande G, et al. The BCR/ABL tyrosine kinase induces production of reactive oxygen species in hematopoietic cells. J Biol Chem. 2000;275:24273-24278.
4. Huang RP, Wu JX, Fan Y, Adamson ED. UV activates growth factor receptors via reactive oxygen intermediates. J Cell Biol. 1996;133:211-220.
5. Sattler M, Winkler T, Verma S, et al. Hematopoietic growth factors signal through the formation of reactive oxygen species. Blood. 1999;93:2928-2935.
6. Ohba M, Shibanuma M, Kuroki T, Nose K. Production of hydrogen peroxide by transforming growth factor-beta 1 and its involvement in induction of egr-1 in mouse osteoblastic cells. J Cell Biol. 1994;126:1079-1088.
7. Utsumi T, Klostergaard J, Akimaru K, Edashige K, Sato EF, Utsumi K. Modulation of TNF-alpha-priming and stimulation-dependent superoxide generation in human neutrophils by protein kinase inhibitors. Arch Biochem Biophys. 1992;294:271-278.
8. Kanbara T, Tomoda MK, Sato EF, Ueda W, Manabe M. Lidocaine inhibits priming and protein tyrosine phosphorylation of human peripheral neutrophils. Biochem Pharmacol. 1993;45:1593-1598.
9. Yuan X, Cong Y, Hao J, et al. Regulation of LIP level and ROS formation through interaction of H-ferritin with G-CSF receptor. J Mol Biol. 2004; 339:131-144.
10. Babior BM, Lambeth JD, Nauseef W. The neutrophil NADPH oxidase. Arch Biochem Biophys. 2002;397:342-344.
11. Sumimoto H, Kage Y, Nunoi H, et al. Role of Src homology 3 domains in assembly and activation of the phagocyte NADPH oxidase. Proc Natl Acad Sci U S A. 1994;91:5345-5349.
12. Sumimoto H, Hata K, Mizuki K, et al. Assembly and activation of the phagocyte NADPH oxidase. Specific interaction of the N-terminal Src homology 3 domain of p47phox with p22phox is required for activation of the NADPH oxidase. J Biol Chem. 1996;271:22152-22158.
13. Heyworth PG, Curnutte JT, Nauseef WM, et al. Neutrophil nicotinamide adenine dinucleotide phosphate oxidase assembly. Translocation of p47-phox and p67-phox requires interaction between p47-phox and cytochrome b558. J Clin Invest. 1991;87:352-356.
14. Touyz RM. Reactive oxygen species in vascular biology: role in arterial hypertension. Expert Rev Cardiovasc Ther. 2003;1:91-106.
15. Corey SJ, Dombrosky-Ferlan PM, Zuo S, et al. Requirement of Src kinase Lyn for induction of DNA synthesis by granulocyte colony-stimulating factor. J Biol Chem. 1998;273:3230-3235.
16. Corey SJ, Burkhardt AL, Bolen JB, Geahlen RL, Tkatch LS, Tweardy DJ. Granulocyte colony-stimulating factor receptor signaling involves the formation of a three-component complex with Lyn and Syk protein-tyrosine kinases. Proc Natl Acad Sci U S A. 1994;91:4683-4687.
17. Zhu QS, Robinson LJ, Roginskaya V, Corey SJ. G-CSF–induced tyrosine phosphorylation of Gab2 is Lyn kinase dependent and associated with enhanced Akt and differentiative, not proliferative, responses. Blood. 2004;103:3305-3312.
18. Gardai S, Whitlock BB, Helgason C, et al. Activation of SHIP by NADPH oxidase-stimulated Lyn leads to enhanced apoptosis in neutrophils. J Biol Chem. 2002;277:5236-5246.
19. Bates RC, Edwards NS, Burns GF, Fisher DE. A CD44 survival pathway triggers chemoresistance via lyn kinase and phosphoinositide 3-kinase/Akt in colon carcinoma cells. Cancer Res. 2001;61: 5275-5283.
20. Baran CP, Tridandapani S, Helgason CD, Humphries RK, Krystal G, Marsh CB. The inositol 5′-phosphatase SHIP-1 and the Src kinase Lyn negatively regulate macrophage colony-stimulating factor-induced Akt activity. J Biol Chem. 2003; 278:38628-38636.
21. Grishin A, Sinha S, Roginskaya V, et al. Involvement of Shc and Cbl-PI 3-kinase in Lyn-dependent proliferative signaling pathways for G-CSF. Oncogene. 2000;19:97-105.
22. Kuroki M, O'Flaherty JT. Extracellular signal-regulated protein kinase (ERK)-dependent and ERK-independent pathways target STAT3 on serine-727 in human neutrophils stimulated by chemotactic factors and cytokines. Biochem J. 1999;341(Pt 3):691-696.
23. Dong F, Gutkind JS, Larner AC. Granulocyte colony-stimulating factor induces ERK5 activation, which is differentially regulated by protein-tyrosine kinases and protein kinase C. Regulation of cell proliferation and survival. J Biol Chem. 2001;276:10811-10816.
24. Wei S, Liu JH, Epling-Burnette PK, et al. IL-2 induces the association of IL-2Rbeta, lyn, and MAP kinase ERK-1 in human neutrophils. Immunobiology. 2000;202:363-382.
25. Mukundan L, Milhorn DM, Matta B, Suttles J. CD40-mediated activation of vascular smooth muscle cell chemokine production through a Src-initiated, MAPK-dependent pathway. Cell Signal. 2004;16:375-384.
26. Chen Q, Powell DW, Rane MJ, et al. Akt phosphorylates p47phox and mediates respiratory burst activity in human neutrophils. J Immunol. 2003;170:5302-5308.

27. Hoyal CR, Gutierrez A, Young BM, et al. Modulation of p47PHOX activity by site-specific phosphorylation: Akt-dependent activation of the NADPH oxidase. Proc Natl Acad Sci U S A. 2003; 100:5130-5135.
28. Sano M, Fukuda K, Sato T, et al. ERK and p38 MAPK, but not NF-kappaB, are critically involved in reactive oxygen species-mediated induction of IL-6 by angiotensin II in cardiac fibroblasts. Circ Res. 2001;89:661-669.
29. El Benna J, Han J, Park JW, Schmid E, Ulevitch RJ, Babior BM. Activation of p38 in stimulated human neutrophils: phosphorylation of the oxidase component p47phox by p38 and ERK but not by JNK. Arch Biochem Biophys. 1996;334: 395-400.
30. Laplante MA, Wu R, El Midaoui A, de Champlain J. NAD(P)H oxidase activation by angiotensin II is dependent on p42/44 ERK-MAPK pathway activation in rat's vascular smooth muscle cells. J Hypertens. 2003;21:927-936.
31. Wang FS, Wang CJ, Chen YJ, et al. Ras induction of superoxide activates ERK-dependent angiogenic transcription factor HIF-1alpha and VEGF-A expression in shock wave-stimulated osteoblasts. J Biol Chem. 2004;279:10331-10337.
32. Noursadeghi M, Bickerstaff MC, Herbert J, Moyes D, Cohen J, Pepys MB. Production of granulocyte colony-stimulating factor in the nonspecific acute phase response enhances host resistance to bacterial infection. J Immunol. 2002;169:913-919.
33. Esposito F, Chirico G, Montesano Gesualdi N, et al. Protein kinase B activation by reactive oxygen species is independent of tyrosine kinase receptor phosphorylation and requires SRC activity. J Biol Chem. 2003;278:20828-20834.
34. Fazal N, Al-Ghoul WM, Schmidt MJ, Choudhry MA, Sayeed MM. Lyn- and ERK-mediated vs. Ca^{2+}-mediated neutrophil O responses with thermal injury. Am J Physiol Cell Physiol. 2002;283: C1469–1479.
35. Oldenburg O, Critz SD, Cohen MV, Downey JM. Acetylcholine-induced production of reactive oxygen species in adult rabbit ventricular myocytes is dependent on phosphatidylinositol 3- and Src-kinase activation and mitochondrial K(ATP) channel opening. J Mol Cell Cardiol. 2003;35:653-660.
36. Dong F, Larner AC. Activation of Akt kinase by granulocyte colony-stimulating factor (G-CSF): evidence for the role of a tyrosine kinase activity distinct from the Janus kinases. Blood. 2000;95: 1656-1662.
37. Dong F, Qiu Y, Yi T, Touw IP, Larner AC. The carboxyl terminus of the granulocyte colony-stimulating factor receptor, truncated in patients with severe congenital neutropenia/acute myeloid leukemia, is required for SH2-containing phosphatase-1 suppression of Stat activation. J Immunol. 2001;167:6447-6452.
38. Qin S, Chock PB. Implication of phosphatidylinositol 3-kinase membrane recruitment in hydrogen peroxide-induced activation of PI3K and Akt. Biochemistry. 2003;42:2995-3003.
39. Seo JH, Ahn Y, Lee SR, Yeol Yeo C, Chung Hur K. The major target of the endogenously generated reactive oxygen species in response to insulin stimulation is phosphatase and tensin homolog and not phosphoinositide-3 kinase (PI-3 kinase) in the PI-3 kinase/Akt pathway. Mol Biol Cell. 2005;16:348-357.
40. Hunter MG, Avalos BR. Phosphatidylinositol 3′-kinase and SH2-containing inositol phosphatase (SHIP) are recruited by distinct positive and negative growth-regulatory domains in the granulocyte colony-stimulating factor receptor. J Immunol. 1998;160:4979-4987.
41. Kitagawa S, Yuo A, Souza LM, Saito M, Miura Y, Takaku F. Recombinant human granulocyte colony-stimulating factor enhances superoxide release in human granulocytes stimulated by the chemotactic peptide. Biochem Biophys Res Commun. 1987;144:1143-1146.
42. Tanimura M, Kobuchi H, Utsumi T, et al. Neutrophil priming by granulocyte colony stimulating factor and its modulation by protein kinase inhibitors. Biochem Pharmacol. 1992;44:1045-1052.
43. Mansfield PJ, Hinkovska-Galcheva V, Shayman JA, Boxer LA. Granulocyte colony-stimulating factor primes NADPH oxidase in neutrophils through translocation of cytochrome b(558) by gelatinase-granule release. J Lab Clin Med. 2002;140:9-16.
44. Mansfield PJ, Hinkovska-Galcheva V, Carey SS, Shayman JA, Boxer LA. Regulation of polymorphonuclear leukocyte degranulation and oxidant production by ceramide through inhibition of phospholipase D. Blood. 2002;99:1434-1441.
45. Ward AC, van Aesch YM, Schelen AM, Touw IP. Defective internalization and sustained activation of truncated granulocyte colony-stimulating factor receptor found in severe congenital neutropenia/acute myeloid leukemia. Blood. 1999;93:447-458.
46. Hermans MH, Antonissen C, Ward AC, Mayen AE, Ploemacher RE, Touw IP. Sustained receptor activation and hyperproliferation in response to granulocyte colony-stimulating factor (G-CSF) in mice with a severe congenital neutropenia/acute myeloid leukemia-derived mutation in the G-CSF receptor gene. J Exp Med. 1999;189:683-692.
47. Kim JH, Chu SC, Gramlich JL, et al. Activation of the PI3K/mTOR pathway by BCR-ABL contributes to increased production of reactive oxygen species. Blood. 2005;105:1717-1723.
48. Sattler M, Mohi MG, Pride YB, et al. Critical role for Gab2 in transformation by BCR/ABL. Cancer Cell. 2002;1:479-492.